Archaeological and Anthropological Sciences (2023) 15:59
https://doi.org/10.1007/s12520-023-01760-1

RESEARCH

Wild or domestic? A 3D approach applied to crania to revisit the identification of mummified canids from ancient Egypt

C. Brassard[1,2] · A. Evin[3] · C. Ameen[4] · S. Curth[5] · M. Michaud[6] · D. Tamagnini[7,8] · K. Dobney[9,10,11,12] · C. Guintard[13,14] · S. Porcier[15] · H. Jerbi[16]

Received: 7 October 2022 / Accepted: 4 April 2023 / Published online: 15 April 2023

Abstract

Many of the millions of animals dedicated to the deities in Ancient Egypt were canids. In contrast to the rare textual sources, the abundance of skeletal remains offers the opportunity to address the question of whether wild or domestic canids were mummified. However, species identification from osteological material remains problematic because it relies on a simple qualitative appreciation or traditional biometric analyses with low discriminatory power, often paired with incomplete comparative reference samples. Here we propose a new method of identification based on cranial form using a 3D landmark–based geometric morphometric approach (GMM). We built predictive methods using a large reference sample of numerical models of crania of modern canids, including a variety of domestic breeds ($N=69$, 38 different breeds) as well as feral dogs ($N=31$), and all species of wild canids present in Africa or the Near East and likely to have been present in Ancient Egypt ($N=157$). We then applied these methods to a sample of ancient canid remains ($N=41$). We compared the effectiveness of multivariate discriminant analyses based on 3D GMM to that using traditional linear morphometric measurements (LMM) commonly taken in the field by archaeozoologists. GMM performs better than LMM in determining the domestic/wild status with cross-validation percentages reaching over 97.5%, and in determining the species among a reduced sample of wild canids with a 96.4% rate (versus 88.2% and 85.2% in LMM respectively). With 3D GMM, we detected the presence of dogs, but also African golden wolves and, for the first time, Near Eastern grey wolves among the mummies.

Keywords Animal mummification · Dog · Ancient Egypt · Geometric morphometrics · Species determination

Introduction

From the 1st millennium BC to the fourth century AD (Roman period), ancient Egyptians mummified millions of animals, including ibises, owls, snakes, crocodiles, fish, cats, and dogs (Murnane et al. 2000; Ikram 2013; Kitagawa 2016; Porcier et al. 2019). Some of these animals had a special status, which implied that their bodies were treated for post-mortem survival much like humans, yet most were classified as 'votive offerings ' to gods and goddesses by Egyptologists. Among those, millions of mummified canids have been discovered throughout Egypt (Dunand et al. 2005, 2017; Ikram 2013; Kitagawa 2016). They were dedicated to the deities of Anubis and Wepwawet (depicted as a canid or a human with a canid head), which were associated with death and travel, recalling wild nocturnal canids (or feral dogs) that roamed human cemeteries (Brixhe 2019).

The precise identity of these two canid deities remains uncertain, however: i.e. whether each god depicts a wild canid or a domestic dog is still debated (Thiringer 2020). Numerous authors have identified Wepwawet as a wolf (*Canis lupus*), perhaps because it was sometimes depicted with white or grey fur (Thiringer 2020), or because the ancient Greeks named Asyut (one of the most well-documented dog necropolises) "Lycopolis" (city of wolf) in its honour. Others identify Wepwawet as a "jackal", referring to depictions showing triangular pointed ears, long bodies, and straight bushy tails. However, these representations may be somewhat misleading as the ancient Egyptians included symbolic codes in such depictions. For example, when represented, jackals are completely black (which corresponds to no known living species of jackals), likely because this color represented regeneration and was associated with Anubis (Schenkel 1963, 2007; Thiringer

✉ C. Brassard
co.brassard@gmail.com

Extended author information available on the last page of the article

2020). The distinction between wild species from art and text is therefore complex in ancient Egypt, where different perceptions of the taxonomic diversity associated with such symbolism likely existed. In all cases, however, a distinction between wild and domestic animals seemed important as they are frequently represented in opposing positions. For example, in the Middle Kingdom and Second Intermediate Period, the board game called 'Hounds and Jackals' was popular (Thiringer 2020).

This singular religious phenomenon, and the uncertainty surrounding the identity of the deities, thus raises a simple question: which canids were used for mummification? Whether wild canids or domestic dogs are represented in mummified offerings will provide insight into e.g. supply strategies (animals bred on purpose, captured from the natural environment, or imported as exotics) and the relative importance of each in the religious practises of ancient Egyptians.

Unfortunately, texts describing practises surrounding canid mummification are scarce, being limited to rare and obscure epigraphic sources dating to the Greco-Roman period. For example, the *Jumilhac papyrus* (332 to 30 BC) testifies that three kinds of canids were protected and venerated, yet they were the subject of ambiguous considerations. Two types of tjesem (tjesem is the ancient Egyptian name for "hunting dog", and it is used to designate a type of greyhound-like dog) are described, but only one was given a proper burial and reached a religious status, the other had its body burned and its ba (i.e. soul, spirit) annihilated after death. A jackal ("ounech") is also described, and its death was the object of celebrations because it was considered an enemy of Osiris (Durisch Gauthier 2002; Bouvier-Closse 2003; Rouvière 2017). Strabon, in his geography, indicates that "a cult and a gift of sacred food" existed for dogs at Cynopolis, which may have been generalized to all of Egypt (Yoyotte et al. 1997). Yoyotte et al. 1997, p. 152) even suggested that pharaohs and some private persons had established agricultural domains whose income ensured the feeding of sacred animals and the maintenance of the priestly personnel assigned to their cults.

Given the scarcity of epigraphic documentation, and the diverse and ambiguous nature of artistic representations, it appears that the zooarchaeological record offers us an alternative way of addressing the question of what canids were mummified. Based on age-at-death data (most canid remains are from very young animals) and the frequent dental anomalies and pathologies observed on these remains, it has been proposed by both Egyptologists and archaeologists alike that most canid mummies were likely domestic dogs, deliberately bred for sacrifice by dedicated keepers (Dunand et al. 2005). Breeding dogs in captivity for sacrifice would have secured a steady and reliable supply of specimens, affording opportunities to satisfy the high demand from pilgrims, and allowing such practises to operate at a large scale. However, wild canids were also occasionally collected (yet it is not clear whether after natural death or intentionally hunted), as attested by recovery of the bones of red or Ruppel's fox (*Vulpes vulpes* and *V. rueppellii*, respectively) and "jackal" from previous excavations (Kitagawa 2016; Brassard 2017; Dunand et al. 2017; Hartley 2017).

The identification of "jackal" in previous studies is somewhat problematic. A number of jackal species are native to Egypt and the surrounding region, including the golden wolf (*Canis lupaster*), the Ethiopian wolf (*Canis simensis*), the side-striped jackal (*Lupulella adustus*), the black-backed jackal (*Lupulella mesomelas*), and the Near Eastern golden jackal (*C. aureus*). To date, conventional wisdom classified Egyptian jackals as a subspecies of the golden jackal (*Canis aureus*; Wilson and Reeder 2005, pp. 574–575). However, recent genetic studies have revealed that they most likely derive from another species altogether, one more closely related to the grey wolf. Whilst studies first suggested that African specimens belong to a cryptic subspecies of the grey wolf (*Canis lupus lupaster*; Rueness et al. 2011; Viranta et al. 2017), others posited they are a completely distinct species (the African golden wolf *Canis lupaster* also referred as *Canis anthus*), showing morphological convergence with Eurasian golden jackals (Koepfli et al. 2015). More recent whole-genome analyses have suggested that it may well be a hybrid of the grey wolf and the 'Ethiopian wolf' (*Canis simensis*; Gopalakrishnan et al. 2018). Given that Egypt is at the crossroads between Africa and the Near East (where the golden jackal is present), it is possible that the Eurasian golden jackal and the African golden wolf are both present in modern and ancient Egypt (Viranta et al. 2017). Moreover, other species of jackals are also present in other geographically close regions—for example the side-striped jackal (*Lupulella adustus*), or the black-backed jackal (*Lupulella mesomelas*); and should, therefore, be considered when assessing species identification from canid bones and mummies. Moreover, although there is no evidence that they have ever lived in Egypt, grey wolves from the Near or Middle East (corresponding to *C. l. pallipes* and *C. l. arabs* subspecies) may have been present among mummified canids, given the geographic proximity with Egypt and the ability of these animals to travel long distances (Castelló 2018) or to be imported along well-established trade routes. It is, therefore, important to revisit conventions of how we determine and categorize "dog/jackal" from zooarchaeological and mummified canids from Egypt, by including in our analyses comparative specimens of all the species likely to be found in Egypt.

Finally, the extent to which imported 'exotic' canids may have been used is still unknown. For example, though the African wild dog (*Lycaon pictus*) was unmistakably represented on carved monumental palettes during the Predynastic period (and only rarely during the Dynastic Period;

Osborn and Osbornová 1998, p. 80), no osteological evidence supports its presence anywhere in the Egyptian territory (Brémont 2021). It is thus possible that it was imported from elsewhere in Africa. Indeed, animals were often represented in Egyptian art despite not being indigenous (e.g. fallow deer, baboon, or elephant; Brémont 2021).

The current methods of determination of bones are problematic for several reasons. To date, the precise identification of canid species has relied on a macroscopic osteological description of bones, mainly skulls, mostly based on qualitative criteria (seeLortet and Gaillard 1903, 1907; Kitagawa 2016; Dunand et al. 2017; Hartley 2017). Measurements taken with callipers are also common, yet the exploration of the trends in these metrics is often limited to bivariate graphs or estimates of wither heights despite the availability of more advanced multivariate analytical methods (Brassard et al. 2021; Callou in Dunand et al. 2017). Moreover, these previous studies unfortunately did not include all possible species of modern canids present in Africa or the Near East. Therefore, it is possible that some wild canids have remained undetected and that their prevalence in faunal assemblages of mummified canids could be more important than previously thought. The present study is the first to consider the full suite of wild and domestic canids likely present in the study region and will help establish a methodology for separating domestic dogs from wild canids.

To date, studies of mummified Egyptian canids have not included an examination of cranial size and shape using 3D geometric morphometrics (3D GMM). This technique consists of analyzing the 3D coordinates of anatomical points called landmarks on the external surface of the object in order to describe its size and shape. The 3D GMM approach allows for a more thorough description and statistical analyses of shape and has proven its ability to differentiate wild and domestic canids in other contexts (Drake et al. 2017; Ameen et al. 2019; Manin and Evin 2020) or other taxonomically close species of mammals such as sheep and goats (Evin et al. 2022; Jeanjean et al. 2022). Advances in 3D data acquisition such as photogrammetry (the basic principle of which is to build a 3D model of the object from 2D photographs) allow easy and cheap data acquisition directly in the field or on museum collections (Evin et al. 2016; Fau et al. 2016). This technique is particularly promising for Egyptian zooarchaeological studies since transporting archaeological remains from the site or between administrative territories within Egypt is forbidden under cultural heritage laws, thus strongly limiting analytical techniques that cannot be undertaken in the field. Photogrammetry in Egyptian archaeological contexts has been limited to human mummies, artefacts, monuments, and even sites (e.g.Lima et al. 2018; Prada and Wordsworth 2018; Abdelaziz and Elsayed 2019; Vasilyev et al. 2019). This is the first study to apply this technique to the examination of animal mummies.

In this study, we propose a novel 3D GMM–based method for the identification of canid species from mummified remains, and above all the domestic versus wild status of these canids, based on cranial shape and size. We focus on complete crania (i.e. skull without the mandible) which are abundant and often very well preserved in dog catacombs or museum collections. Moreover, their shape carries a strong phylogenetic signal (making it one of the elements for which species diagnosis is easiest). First, we assess the ability of cranial shape and size to distinguish between modern canids of known species, including a dataset of domestic dogs incorporating dogs of known breeds as well as feral specimens. We further sampled wild canid species present in Africa or the Near East and likely to have been present or possibly imported into Ancient Egypt. We then applied predictive methods on a small sample of ancient canid remains from different dog catacombs found along the Nile valley and maintained in the collections in the Musée des Confluences in Lyon (France). We used multivariate statistics to optimize the exploitation of metric data, and compared the effectiveness of discriminant analyses based on 3D geometric morphometrics with that based on traditional morphometrics using linear measurements. Although a few studies have suggested that linear measurements are not accurate for dog/wolf identification (e.g. Drake et al. 2015), detailed differences with other species remain to be explored, especially in the context of ancient Egyptian mummies. In addition, many canid remains were previously studied directly in the field by taking linear measurements with callipers and whilst a great amount of data are available (e.g. Kitagawa 2016; Dunand et al. 2017; Hartley 2017), the studied specimens are no longer accessible today and new data cannot be generated with another method. A determination method based on linear morphometrics would thus allow to revisit the identification of these ancient canid mummies, based on previously recorded quantitative data. To do so, we used both linear and geometric morphometric analyses commonly used in evolutionary biology or zooarchaeology allowing us to assess the morphological variation and to discriminate between putative species before predicting the identification of the ancient remains (e.g. seeClaude 2013; Fabre et al. 2014; Evin et al. 2020; Parés-Casanova et al. 2020; Jeanjean et al. 2022).

Materials

Modern reference sample

We investigated a total of 257 crania of modern canids collected from several institutions (detailed information about the origin and constitution of this sample is provided in SI 1). Wild canids are represented by 157 specimens from 13 species of the genus *Canis*, *Lupulella*,

Lycaon, *Otocyon*, and *Vulpes* (Table 1). Modern domestic dogs are represented by 100 specimens from a minimum of 38 different breeds (some pure, and others being crossbreeds). Based on the assumption that ancient dogs may be similar in shape to medium-headed modern dogs rather than breeds with highly specialised morphologies, we included in this sample 26 modern feral dogs from Tunisia, Egypt, and Turkey, as well as 5 modern beagles, whose skull shape is average among modern breeds (see Brassard et al. 2022). We also included long-headed dogs (i.e. dolichocephalic dogs, such as greyhounds, Afghan hounds) and short-headed dogs (i.e. brachycephalic dogs, such as Bullmastiffs, Boxers) to account for a full range of domestic variability within our analyses. We estimated how long- or short-headed the modern dogs are by calculating their cranial width (measurement taken between the zygomatic arches which corresponds to measurement CR30 in Fig. 1) and length ratios (CR1), which corresponds to the cephalic index CI (CI = CR30/CR1, Roberts et al. 2010). We arbitrarily choose the cut-off values, to obtain balanced groups: dogs with a CI ≥ 0.55 were considered brachycephalic, dogs with a CI ≤ 0.50 were considered dolichocephalic, and dogs with an intermediate CI were considered mesocephalic.

We only considered subadult, young, and adult specimens, with permanent teeth fully erupted (i.e. excluding the juveniles). This limits ontogenetic variation since age is known to have a significant impact on skull morphology, which is all the more important in sexually immature canids (i.e. before 8–12 months, see Forbes-Harper et al. 2017; Brassard 2020). Specimens were divided into categories depending on the degree of closure of the cranial sutures (Barone 2010). We considered as subadults specimens with all the permanent teeth erupted but a suture between the basisphenoid and the basioccipital (*synchondrosis sphenooccipitalis*) still open (between 6 and 8/10 months). We categorized specimens as young if the suture between the basisphenoid and presphenoid was not completely closed (between 10 months and 1–2 years old). Specimens were classified as adult if the basisphenoid and presphenoid suture was completely closed (more than 1–2 years old). When the suture between the basisphenoid and the presphenoid was not clearly visible, individuals were classified as 'young/adult?'. Subadults are sexually immature specimens, but we chose to keep them in the analyses as we want to propose a method with the widest possible range of application (in terms of age).

Our aim is not to assess morphological differences between age and sex categories. However, we were careful to provide a reference sample that was as comprehensive and balanced as possible. As such, there are fewer subadults than adults in the sample, but their presence will help identify subadults in the archaeological sample.

Table 1 Constitution of the modern sample in terms of species, breed, sex, and age at death. Sex information, when available, is provided in brackets as follows (female/male)

Species	Breed	*N*	By age			
			Subadults	Young	Adults	Young/adults?
Canis familiaris	Total including	100 (32.34)	10 (5.3)	31 (8.15)	35 (14.10)	24 (2.5)
	Feral	31 (13.15)	6 (6.3)	13 (4.7)	8 (6.2)	4 (0.3)
	Beagles	5 (3.2)	0	1 (1.0)	4 (2.2)	0
	Brachycephalic	28	1	11	16	0
	Mesocephalic	32	2	9	13	8
	Dolichocephalic	40	7	12	14	7
Canis lupus		16	3 (1.1)	11 (2.3)	0	2
Canis lupaster		17	1 (0.0)	10 (4.4)	4 (2.1)	2 (1.1)
Canis aureus		2	0	2 (0.1)	0	0
Canis simensis		9	1 (0.0)	8 (2.2)	0	0
Lycaon pictus		13	1 (1.0)	6 (2.2)	4 (0.1)	2 (0.1)
Lupulella mesomelas		20	4 (1.2)	10 (1.1)	1 (0.0)	5 (2.2)
Lupulella adustus		8	0	4 (4.0)	1 (1.0)	3 (0.3)
Vulpes vulpes		23	3 (1.1)	8 (3.2)	3 (1.1)	7 (1.3)
Vulpes rueppellii		15	1 (0.0)	2 (1.0)	12 (2.5)	0
Vulpes pallida		10	1 (0.1)	2 (0.2)	4 (2.2)	3 (0.1)
Vulpes chama		4	0	0	2 (0.0)	2 (0.2)
Vulpes zerda		13	1 (1.0)	3 (1.1)	4 (1.0)	5 (0.1)
Otocyon megalotis		7	0	0	4 (1.3)	3 (1.2)
total of the modern sample		**257**	**24 (10.7)**	**88 (28.30)**	**77 (26.24)**	**56 (7.21)**
Ancient mummies		**41**	**7**	**7 (2.2)**	**14 (1.0)**	**13 (1.1)**

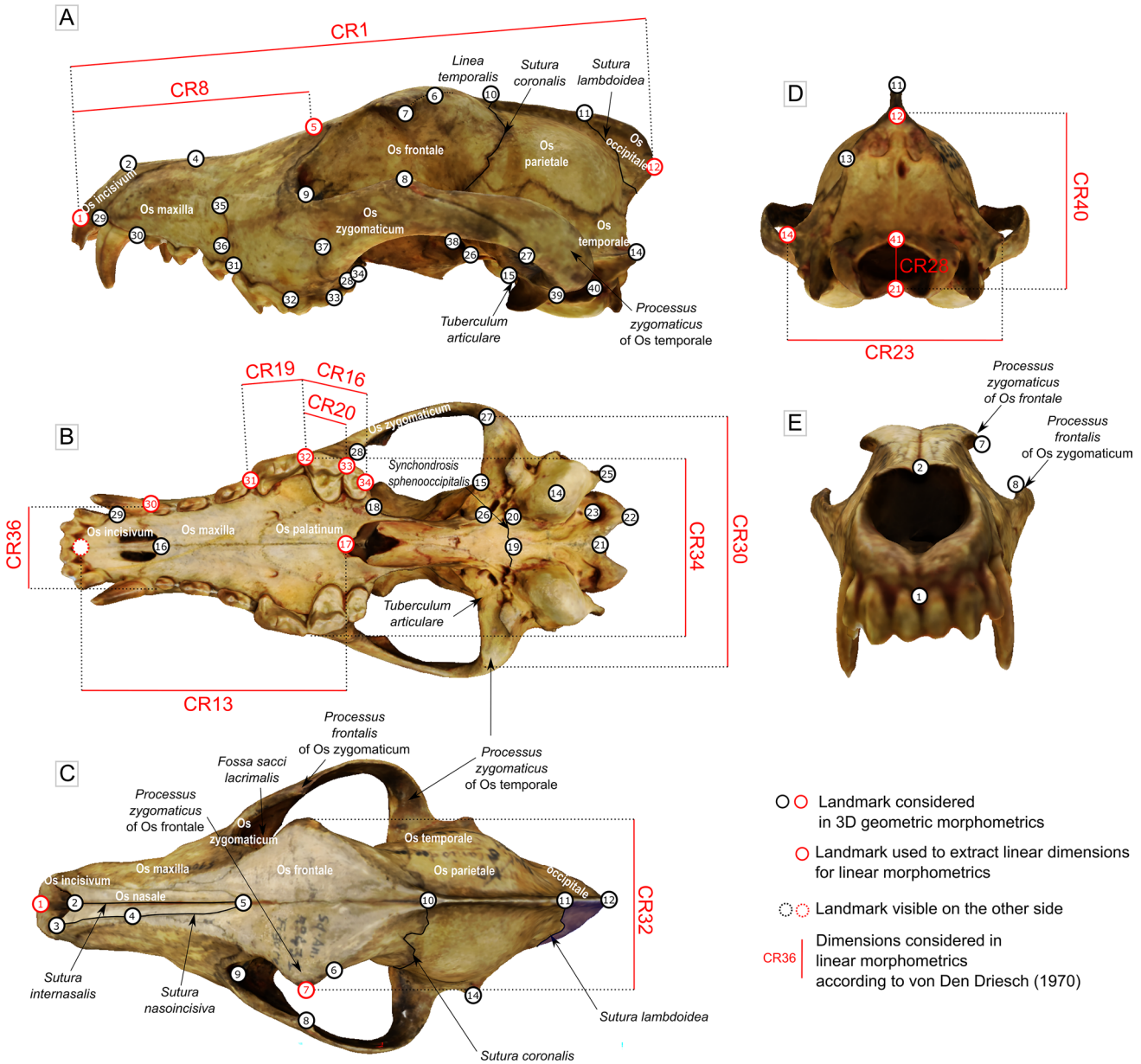

Fig. 1 Geometric and linear morphometric protocols: position of the landmarks captured on the cranium, and correspondence with the linear dimensions considered in our analyses according to von den Driesch (1976). Landmark positions and linear measurement are described in Tables 2 and 3, respectively. Anatomical features mentioned in Table 2 are indicated. **A** lateral view, **B** ventral view, **C** dorsal view, **D** caudal view, **E** rostral view

Archaeological specimens

We analyzed 41 archaeological crania from ancient canid mummies collected in dog catacombs along the Nile Valley by Louis Lortet, Claude Gaillard, and Gaston Maspéro in the early twentieth century. No precise date is available for these specimens, but some other dog mummies from the collection were radiocarbon dated, and the oldest date to the 30th Dynasty, around 360 BC (Richardin et al. 2017; Porcier et al. 2019). Geographic provenance is known only for 26 specimens; these are from Assiout, Assouan, Rôda, Saqqara, Tehneh, and Thebes (Louqsor; see SI 1). Some identifications were proposed by previous authors (Lortet and Gaillard 1903, 1907), and are compared with the identification obtained in our study.

Only specimens without pathological or taphonomic deformation of at least one side of the braincase were included in shape analyses. Several specimens showed dental anomalies (in particular tooth absence with healed alveolus, or advanced signs of periodontal disease

characterized by osteolysis near the tooth alveolus, for example in CCEC.51000031, see SI2 and Supplementary Material). Dental anomalies, when present, did not affect landmark acquisition, however.

Methods

Data acquisition

3D modeling

Scaled 3D models of the crania were obtained from different operators and by different methods, including photogrammetry, surface scanning (Einscan), and medical CT scan protocols (see SI 2 for details). The models were repaired, cleaned, simplified, and mirrored where needed using © 'Geomagic Wrap' (version 2013.0.1.1206) and 'MeshLab' (v2016.12; Cignoni et al. 2008).

3D geometric morphometrics (GMM)

Cranial shape was quantified from the 3D coordinates of landmarks placed by a single operator (first author CB) on the numerical models using the software 'IDAV Landmark', version 3.0.0.6 (©IDAV 2002–2005; Wiley et al. 2005). Forty-one unilateral landmarks were placed on the left side of the cranium (Table 2 and Fig. 1) and were then mirrored for further visualizations, using the function 'mirrorfill' from the package 'paleomorph' in R (R Core Team 2021). The resulting raw coordinates are available in the supplementary material (SI3).

All following analyses were carried out in R, using mainly the packages 'Morpho' (Schlager 2017) and 'Geomorph' (Adams et al. 2016).

Mirrored landmark coordinates were superimposed following a Generalized Procrustes Analysis (GPA) using the function 'procSym' (Rohlf and Slice 1990; Goodall 1991; Mitteroecker and Gunz 2009; Dryden and Mardia 2016). During this procedure, the raw coordinates undergo translation, scaling, and rotation to standardise the relative positioning of the specimens around their centroid to minimize the squared summed distances between corresponding landmarks (Rohlf and Slice 1990). Centroid size (CS) is the square root of the sum of squared distances of the landmarks from their centroid (Bookstein 1991) and measures the dispersion of the landmarks around the centroid. This can be used as a univariate summary of the overall size of the cranium. From this procedure, we extracted the Procrustes coordinates and the log10-transformed centroid size, which are used to describe cranial shape and size, respectively. The new set of shape coordinates obtained from the GPA—namely Procrustes coordinates—together represent the total amount of shape variation in the entire sample. When the analyses focussed only on certain specimens, new GPAs were conducted separately for each separate dataset (corresponding to further analyses, e.g. when considering all species or just some of them).

For visualizations of shape variation, the 3D surface scan of the cranium of a feral dog was warped onto the consensus shape of the GPA, and then deformed using thin-plate spline using the function 'tps3d' (Bookstein 1989).

Linear morphometrics

We chose 13 linear measurements following the nomenclature of von den Driesch (1976) and commonly used by archaeologists and Egyptologists (Table 3 and Fig. 1). To obtain these measurements, we calculated the Euclidean distance to the nearest 1 mm between corresponding 3D landmark coordinates (Table 3). We chose these measurements to represent the length, width, and height of the cranium and avoid measurements that may carry redundant information. To disentangle size and shape from the LMM data (as done in GMM), we used the log-shape ratio method (Mosimann 1970). Following this method, size was computed as the log10 of the geometric mean of all measurements (i.e. isometric size), and shape as the log10 of each measurement divided by the isometric size (shape ratios).

Statistical analyses

To refine our morphometric descriptions and interpretations, we performed analyses on (log10-transformed) size (isometric size in LMM and centroid size in GMM) and shape (shape ratios in LMM and Procrustes coordinates in GMM) separately. Considering that size is an important part of the phenotype that may drive the differences between species and that intraspecific variation related to ontogeny is limited (as we focused on specimens older than 6 months), we did not perform analyses on allometry-free shapes (allometry refers to size-related changes in shape; Klingenberg 2016). Statistical analyses were performed following the same steps for 3D geometric (GMM) and linear morphometrics (LMM). First (step 1), we visualized the overall morphometric cranial variability in the total sample. Then (step 2), we attempted to identify domestic dogs in the archaeological sample by applying a predictive discriminant analysis that separates modern domestic dogs from all the wild species considered together in the modern reference sample. Finally (step 3), we refined the identifications for the specimens identified as wild by running a second predictive discriminant analysis including only a subsample of the wild species. This three-step approach allowed us to conduct statistical analyses on reasonably large sample sizes.

Table 2 Definition of the landmarks used in this study following the Nomina Anatomica Veterinaria nomenclature (NAV, 2017)

Landmark	Definition
1	Most rostral point of Os incisivum, between incisor teeth I1 in dorsal view (Prosthion)
2	Most rostral point of Os nasale, on the midline (sutura internasalis)
3	Most rostral point on sutura nasoincisiva
4	Point at the junction of Os incisivum, Os nasale, and maxilla
5	Most caudal point of Os nasale, on the midline (sutura internasalis), and at the junction with Os temporale (nasion)
6	Most medial point at the postorbital constriction on the curvature corresponding to linea temporalis
7	Most lateral point of the Processus zygomaticus of Os frontale
8	Processus frontalis of Os zygomaticum
9	Most rostral point of the curvature of the lower edge of the fossa sacci lacrimalis
10	Bregmatic fontanel, most medial point of the sutura coronalis, on the midline (Bregma)
11	Most rostral and medial point on the sutura lambdoidea on the midline
12	Most posterior end of Os occipitale (inion, called akrokranion by von den Driesch)
13	Point at the extreme convex curvature of the tuberculum nuchale
14	Point at the extreme convex curvature of the crista supramastoidea
15	Most medial point of the tuberculum articulare of Pars squamosa of Os temporale
16	Most rostral point of maxilla in ventral view, on the midline
17	Most caudal point of Os palatinum, on the midline
18	Caudally to molar tooth M2, in the recess medial to tuber maxillae of Os maxilla (on the facies pterygopalatine)
19	Most caudal point of the synchondrosis sphenooccipitalis, on the midline
20	Most lateral point of the synchondrosis sphenooccipitalis, rostrally to the bulla tympanica
21	Most ventral point of foramen magnum of Os occipitale, on the midline (Basion)
22	Most caudal point of the Condylus occipitalis of Os occipitale in ventral view
23	Point on the Canalis n. hypoglossi of Os occipitale in ventral view
24	Ventral tip of the bulla tympanica
25	Tip of Processus paracondylaris
26	Most dorsal and caudal point of the foramen alare caudale
27	Most ventral and posterior point at the junction of the Processus zygomaticus of Os temporale and Os zygomaticum, on the Arcus zygomaticus
28	Most caudal point at the junction between maxilla and Os zygomaticum, under Arcus zygomaticus, and near the tuber faciale
29	Most cranial point of the alveolus of the canine tooth, on lateral side
30	Most caudal point of the alveolus of the canine tooth, on lateral side
31	Most cranial point of the alveolus of the upper carnassial tooth P4, on lateral side
32	Point between the alveolus of P4 and M1 teeth, on lateral side
33	Point between the alveolus of M1 and M2 teeth, on lateral side
34	Most caudal point of maxilla behind tooth M2
35	Most dorsal point of the foramen infraorbitale
36	Most ventral point of the foramen infraorbitale
37	Most caudal point of curvature at the junction of maxilla and Arcus zygomaticus of Os zygomaticu on lateral side
38	Most ventral and caudal point of the foramen rotundum and alare rostrale
39	Most rostral point of meatus acusticus externus on lateral side
40	Most caudal point of meatus acusticus externus on lateral side
41	Dorsal and caudal border of the foramen magnum, on the midline (opisthion)

Step 1: preliminary visualization of the morphological variability in the modern and archaeological sample

First, we visualized the morphological variability using boxplots for size and principal component analysis (PCA) for shape (we used the function 'prcompfast' and a similar code as the source code of the function 'procSym' to obtain the eigenvalues and scores). PCA reduces the dimensionality of shape data whilst preserving as much of the information contained in the original data as possible. Thus, the first factorial plane, defined by the two first PCA axes, provides a representation of the overall variability in the dataset. The

Table 3 Cranial measurements considered in this study following von den Driesch (1976)

Measurement	Definition	Correspondance with landmarks
cr1	Prosthion–akrokranion	1–12
cr8	Prosthion–nasion	1–5
cr13	Median palatal length: staphylion prosthion	1–17
cr16	Length of the molar row (measured along the alveoli on the buccal side)	32–34
cr19	Length of the carnassial alveolus	31–32
cr20	Length of M1alveolus	32–33
cr23	Greatest mastoid breadth: greatest breadth of the occipital triangle: otion–otion	14–14′
cr28	Height of the foramen magnum: basion–opisthion	21–41
cr30	Zygomatic breadth: zygion–zygion	27–27′
cr32	Frontal breadth: ectorbitale–ectorbitale	7–48
cr34	Greatest palatal breadth: measured across the outer borders of the alveoli	32–32′
cr36	Breadth at the canine alveoli	30–30′
cr40	Height of the occipital triangle: akrokranion–basion	12–21

contribution of linear dimensions to the first axes of the PCA in LMM was visualized using bar plots. In GMM, axes were interpreted based on visualizations and deformations from the consensus to the theoretical shapes at the minimum and maximum of the PC axes (which were computed using the function 'restoreShapes'). The morphological differences between group means were visualized by deformations from the consensus to the mean shape of each species (SI 1). The PCA was calculated based on the Procrustes coordinates of the modern specimens only, before projecting the archaeological specimens as supplementary individuals (using the same source code as in the function 'PCA' from package 'FactoMineR').

We explored differences in shape variability between dogs ($N = 100$) and all wild canids grouped together ($N = 157$) through disparity tests (Foote 1997). The morphological disparity of each group was estimated as the Procrustes variance (i.e. the sum of the diagonal elements of the group covariance matrix divided by the number of observations in the group) using the residuals of a linear model fit (we used the function 'morphol.disparity' with 999 permutations with the formula shape ~ 1 to use the overall mean rather than group means; (Zelditch et al. 2012).

Step 2: identification of the domestic dogs

In this second step, all the wild species were grouped into one group to obtain a larger sample to oppose the domestic group. The aim was to identify the domestic dogs among the archaeological canids.

Differences in cranial shape between wild and domestic groups were tested using MANOVAs (function 'manova') on the scores of the non-zero PC components from the PCA in LMM. In GMM, we performed Procrustes ANOVA on Procrustes coordinates with a residual randomization permutation procedure (using the function 'procD.lm' with 999 iterations and 'RPPP = TRUE'; (Goodall 1991; Collyer et al. 2015).

The discriminatory power of GMM and LMM was also assessed by linear discriminant analyses (LDA) paired with a leave-one-out cross-validation procedure to determine classification accuracy. Classification accuracy corresponds to the percentage of specimens correctly re-assigned to their own group. The leave-one-out procedure removes one specimen at a time and predicts its classification into a priori defined reference groups using the LDA function computed on all the remaining specimens. The procedure is repeated for each specimen in the sample, each in turn being treated as an unknown. This avoids predicting a specimen on the basis of a function computed on data that includes the specimen itself which would tend to spuriously inflate classification accuracy (Kovarovic et al. 2011). A weakness of this method is that it is sensitive to the number of variables, sample size, and unbalanced design (seeMitteroecker and Bookstein 2011; Evin et al. 2013, 2015). By grouping together all the specimens of the wild species ($N = 157$), we avoided the problem of small sample size for some species (e.g. *C. aureus* is only represented by two specimens, Table 1). To avoid the over-fitting of the data caused by the high number of variables and unbalanced design, we performed analyses after dimensionality reduction and homogenization of group samples using the function 'mevolCVP' (Evin et al. 2013). This function allows us to determine the number of PCs needed in order to maximize the differences between groups. We replaced the original shape variables

(Procrustes coordinates or shape ratios) with the scores of these first PCs (Baylac and Frieß 2005; Evin et al. 2013). In this procedure, perfectly balanced groups are obtained by a random selection (repeated 1000 times) of a number of specimens in the largest samples equal to the sample size of the smallest group. The outcomes of this iterative resampling approach were summarized by the upper and lower 95th percentiles of the posterior probabilities of the 1000 balanced LDAs (called herein cross-validation percentage or CVP). To track the reference specimens that are the most difficult to assign to a group, we applied predictive LDA to the same specimens as the one used to build the predictive model. We used the 'pldam' function from Evin et al. (2015) to perform analyses after homogenization of group sizes, with arguments nrep = 1000, limproba = 0, and limCVP = 95% in GMM or 85% in LMM. In other words, each specimen was assigned to a group 1000 times, and the final identification was the most attributed group among the LDAs with a CVP above 0.95 in GMM and 0.85 in LMM, without a cut-off value of the posterior probability at each iteration. We extracted the frequencies of attribution to a group to discuss the robustness of the identifications for each specimen.

The archaeological specimens were then assigned to the wild or domestic group using the same method.

Step 3: identification of the species among the wild group

In step 3, a new superimposition and PCA were performed only with the wild modern specimens and by projecting in the PCA, as supplementary individuals, the archaeological specimens that were classified as wild in step 2 in order to establish the list of the candidate species for further predictions of the wild canids among Egyptian mummies. In further analyses, we included only the wild species that are closest to the archaeological specimens on the first factorial plane of the PCA. We also excluded species with low sample sizes (e.g. *Canis aureus*, $N = 2$). We then tested the differences in mean cranial shape and disparity between the candidate wild species using the same methods as in step 2. The MANOVA in LMM and Procrustes ANOVA in GMM were followed by post hoc tests (function 'pairwise.perm.manova' from package 'RVAideMemoire', and function 'pairwise' from package 'RRPP'). We assessed the discriminatory power of GMM and LMM to distinguish these wild species using the same linear discriminant method as in step 2.

We finally performed a second predictive LDA to determine the species (among *C. familiaris*, *C. lupus*, *C. lupaster*, and *C. mesomelas*) of the archaeological specimens identified as wild by the first LDA. We contrasted our identifications with the range of values in cranial size for each species in the modern sample (illustrated in the boxplot of step 1).

Results

Step 1: variability in dogs compared to wild African canids

Variability in cranial size

Dogs exhibit a large amount of variation in cranial size and strongly overlap with other middle-sized to large canids for both GMM and LMM analyses (Fig. 2), making size alone an insufficient criterion for species identification or the separation of wild from domestic specimens.

Variability in cranial shape

Dogs display as much intra-group variability in cranial shape as all the wild specimens in our study when grouped together, as observable on the two first PCA scores (Fig. 3) and demonstrated by the results of the disparity tests for both GMM and LMM analyses (GMM: $P = 0.042$, Procrustes variance = 0.0061 in 100 dogs and 0.0052 in the 157 wild canids; LMM: $P = 0.4$, Procrustes variance = 12.2 in dogs and 13.5 in wild canids). The GMM analyses even tend to suggest a greater disparity in dogs compared to *C. lupus*, *C. lupaster*, and *L. mesomelas* ($P < 0.003$). Other comparisons are not significant when retaining a P value below 0.01 (see SI 4 for details).

Moreover, we observe that the first factorial plane of the PCA is much less discriminating between domestic and wild species in LMM than for GMM (Fig. 3).

Step 2: distinction between wild and domestic groups and identification of domestic dogs

In both GMM and LMM analyses and when only two categories are considered, domestic dogs and wild canids differ highly in their cranial shape (LMM: $P_{\text{MANOVA}} < 0.001$; GMM: $P_{\text{Procrustes ANOVAs}} < 0.001$, $R^2 = 0.16$).

Discriminant analyses performed in GMM on a balanced sample and a reduced dataset (we kept only the first 12 PCs, which account for only 78.4% of the total variance but are enough to discriminate species according to the results of the 'mevolCVP' function) show that each specimen can be correctly classified between domestic and wild with a global accuracy of 97.5% (95% confidence interval: 97.45–97.54%). When applying predictive LDA to the same specimens as the one used to build the predictive model, all domestic dogs were correctly assigned, but six wolves (out of the 16) and one golden wolf were not correctly assigned (see SI 6). Thus, step 2 identifies 100% of the dogs but it has only 62.5% accuracy for grey wolves (and 94% for golden wolves). As a consequence, when applying this model to an unknown sample, there may still be wolves among the identified dogs.

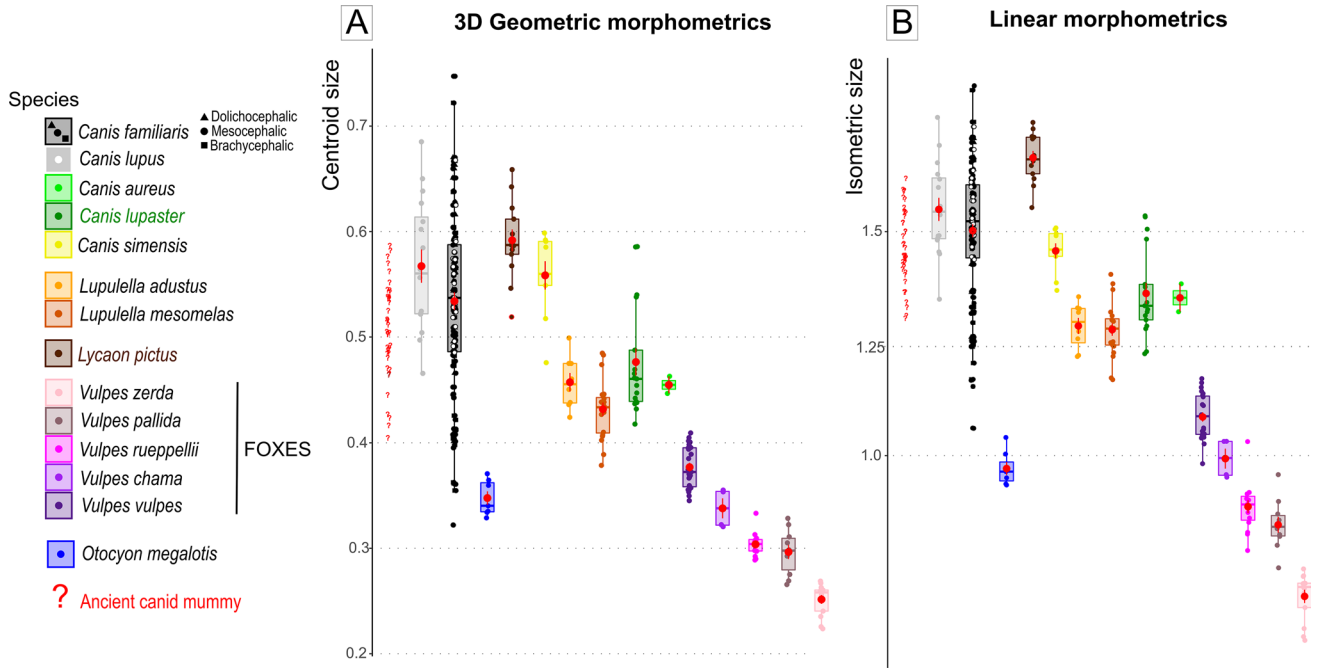

Fig. 2 Visualization on boxplots of the variability in cranial size in modern ($N=100$ dogs and 157 wild specimens) and ancient ($N=41$) canids according to GMM (**A**) and LMM (**B**) analyses. Ancient dogs are represented by red question marks, and modern dogs are in black. Modern wild species are indicated in different colors. Point shape indicates the morphotype of modern dogs. See Table 1 and SI 2 for details about the sample. The red dots and red vertical lines indicate the mean and standard deviation for each group

LMM has less discriminatory power than GMM: the accuracy of the balanced LDA is lower (analysis performed on the first 8 PCs, which represents 93.7% of the total variance: CVP = 88.2% [88.09–88.30%]). Nine dogs were classified as wild and 20 wild canids (including 9 wolves) were identified as domestic (SI 6).

When predicting the domestic status of the archaeological specimens, 33 were identified as domestic dogs and 8 as wild canids in both GMM and LMM analyses. However, the class assignment is different between GMM and LMM analyses for four specimens (Fig. 4A and Table 4). In GMM, the frequency of attribution of all specimens to a group was over 90%. For LMM, this percentage (when considering LDAs with a CVP higher than 85%) was lower, especially for some specimens that were easily classified in GMM (e.g. CCEC.51000010, see SI 6).

Step 3: identification of the species in the wild group

When the eight possible ancient wild canids (identified in step 2) are projected in the first factorial plane of the PCA performed on shape data (GMM) of the modern wild specimens, they position close to *C. lupus*, *C. lupaster*, *C. aureus*, and *C. mesomelas* (Fig. 4B1, B3), which allows us to refine the list of candidate species for further prediction analyses. Moreover, we observe that all ancient canids in our sample have cranial centroid sizes out of the range of *V. zerda*, *V. pallida*, *V. chama*, *V. rueppellii*, and *O. megalotis* in the GMM analyses, and even *V. vulpes* in the LMM analyses (Figs. 2 and 3, SI 5). Size thus supports the exclusion of these species in step 3.

When considering only *C. lupus*, *C. lupaster*, and *L. mesomelas* in our analyses (the sample of *C. aureus* was too small to be included), we find significant differences in the mean cranial shape between the three species in both GMM and LMM analyses (GMM: $P<0.001$, $R^2=0.22$, $P<0.001$ for all post hoc comparisons; LMM: $P<0.001$, $P=0.02$ for all post hoc comparisons). We also observe that *C. lupaster* (Procrustes variance = 0.0017) is less variable in shape than both *C. lupus* (Procrustes variance = 0.0024, $P=0.009$) and *L. mesomelas* (Procrustes variance = 0.0024, $P=0.008$) in GMM analyses (results are not significant in LMM). We also obtain excellent classification rates in GMM analyses with the balanced LDA: more than 96% (96.4% [96.3–96.5%]) performed on the first seven PCs (representing 63% of the total variance). The accuracy is lower in LMM analyses (85.2% [84.9–85.6%] in the balanced LDA on the first 10 PCs).

When considering only *C. lupus*, *C. lupaster*, and *L. mesomelas* in the balanced LDA, 2 canid mummies were identified as *C. lupus* and 6 as *C. lupaster* (Fig. 4C), with a frequency over 98% except for one specimen (Table 4). CCEC.90010304 was indeed attributed to *C. lupus* only in 77% of the LDAs with CVPs higher than 95%. It was identified as *C. lupaster* in 23% of the LDAs (SI6). However, based

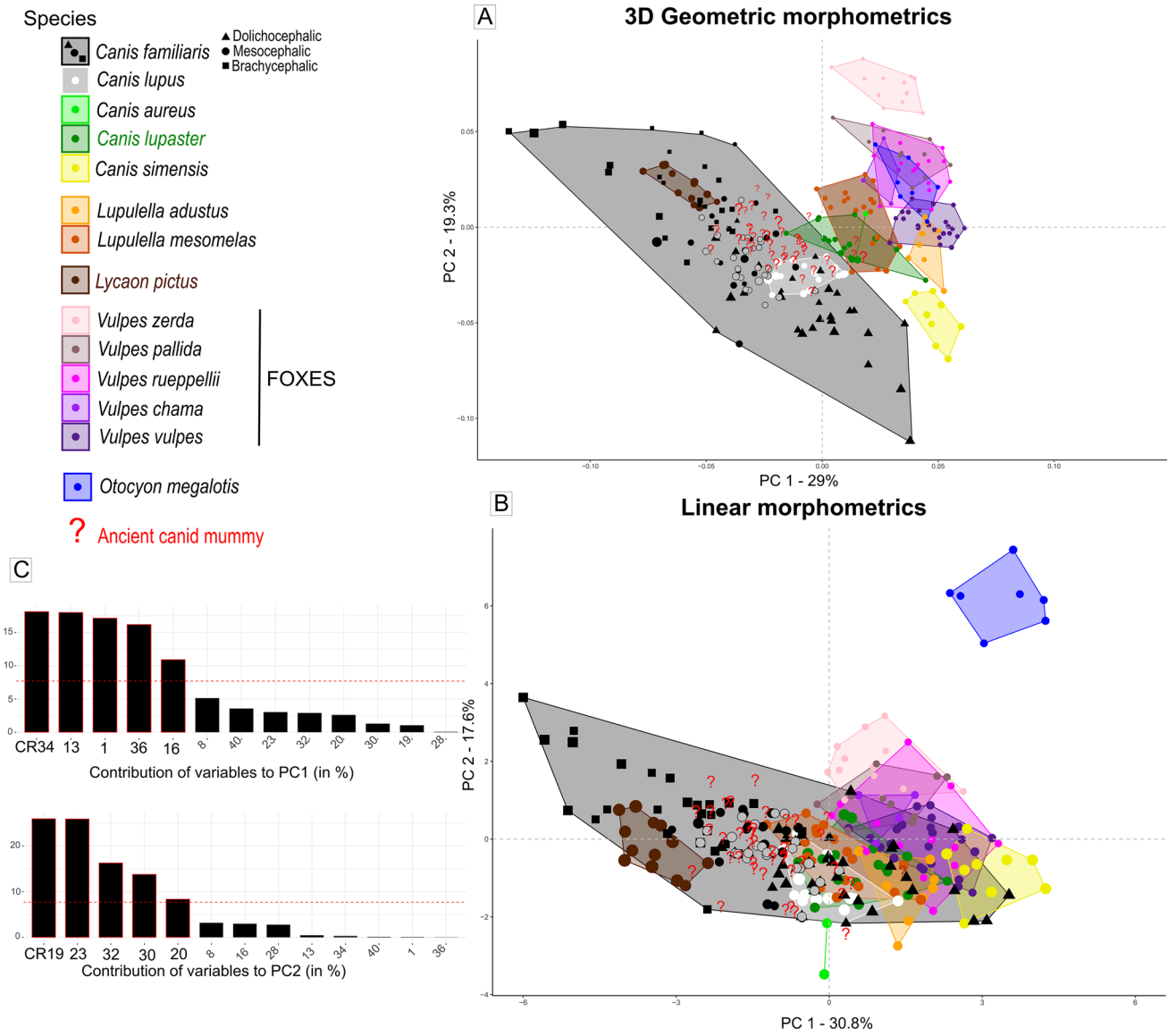

Fig. 3 Visualization of the variability in cranial shape on the first factorial plane of the PCA in modern ($N=100$ dogs and 157 wild specimens) and ancient ($N=41$) canids according to GMM (**A**) and LMM (**B**) analyses. **C** Contribution of linear measurements to PC1 and PC2 in LMM analyses. Icon size is proportional to the log10 of the centroid size. Ancient dogs are represented by red question marks, and modern dogs are in black. Modern wild species are indicated in different colors. Point shape indicates the morphotype of modern dogs. See Table 1 and SI 2 for details about the sample

on its centroid size, it is more likely to be a wolf (SI 5). For the LMM analyses, there is more overlap between the wild species in the PCAs, in particular between *C. lupus* and *C. lupaster* (Fig. 4B2, B4), and five ancient specimens were identified as *C. lupaster* and three as C. *lupus*. Only three specimens are attributed to the same wild species in GMM and LMM (2 *C. lupaster* and 1 C. lupus, Table 4, SI 6). Given the higher ability of GMM to distinguish between domestic and wild canids, and to distinguish between *C. lupus*, *C. lupaster*, and *L. mesomelas*, we consider the attributions related to GMM analyses to be more reliable. All these attributions are compatible with the range of centroid size between species, considering that some specimens are relatively young (Table 4 and Fig. 2). Yet one must note that one specimen identified as a *C. lupaster* has a rather large centroid and isometric sizes compared to modern golden wolves (CCEC. 51000004, SI 5), all the more because it is a young specimen.

In the PCAs, icon size is proportional to the log10 of the centroid size. Ancient dogs are represented by red question marks, and modern wild species are indicated in different colors. See Table 1 and SI 2 for details about the sample, and SI 6 for details about LDA attributions.

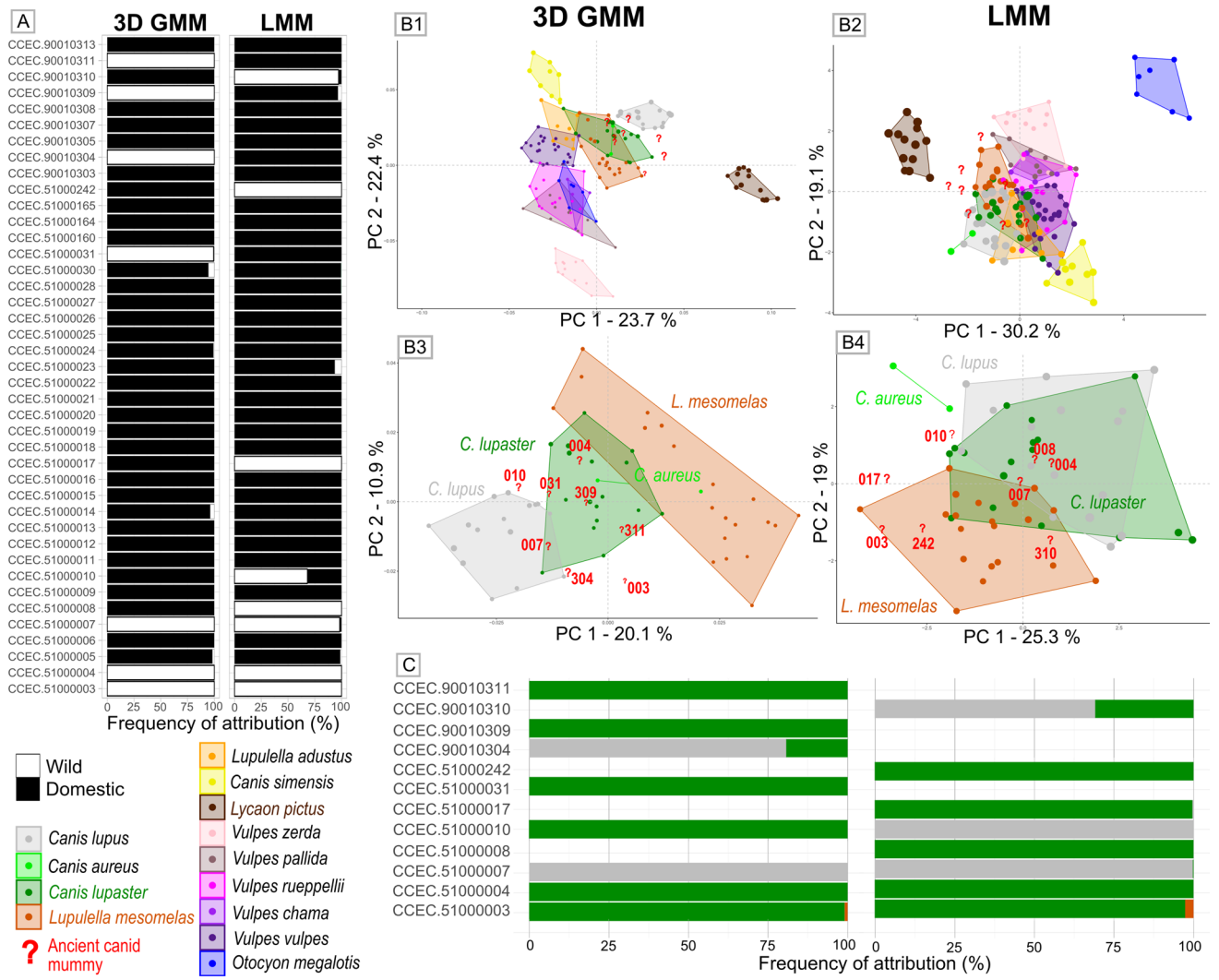

Fig. 4 Comparison of species predictions for archaeological dogs, in GMM versus LMM analyses. A: frequency of attribution between wild and domestic (step 2) during predictive LDA iterations (pldam); B: visualization of the variability in cranial shape on the first factorial plane of the PCA in all ancient ($N=8$) and modern ($N=157$) wild specimens (B1, B2) or on the PCA performed on the candidate species only (B3, B4) according to GMM (B1, B3) and LMM (B2, B4) analyses. C: classification of the wild canid mummies: frequency of attribution between *C. lupus*, *C. lupaster*, and *L. mesomelas* (step 3) during predictive LDA iterations (pldam)

Discussion

Statistical biases related to classification

Although our modern reference sample is representative of all species potentially present in the region, some species are represented by only a few specimens. Consequently, our sample may not fully represent the variability within the species, nor account for past variation not present in extant populations. Several factors come into play here. Some species are particularly difficult to find in collections. For example, we had only one specimen of *Vulpes chama* (but as it is limited to the extreme south of Africa, it is unlikely to be found in ancient mummies) and only two *Canis aureus* (for most specimens identified as golden jackal in the collections, their location suggests that they were in fact *Canis lupaster*). Moreover, we did not find any specimen of bat-eared foxes (*Vulpes cana)* to include in our study. The native range of this species along the Red Sea coastal mountains in eastern Egypt (as well as in the south of the Arabian peninsula and Iran; Castelló 2018, p. 207) makes it a more likely candidate for inclusion in mummified remains than foxes from more geographically distant areas (e.g. the cape fox, *Vulpes chama*). Previous studies suggest that the skull of *V. cana* can be easily distinguished from that of *V. rueppellii* (with which it is sympatric throughout its known African range) by its "smaller size, sharply pointed and relatively long snout" (Saleh et al. 2018, p. 18). It is also larger than

Table 4 Determination of wild canids among ancient specimens based on geometric (GMM) and linear morphometrics (LMM) and confrontation with data about size (Csize), age, dental anomalies, previous determination, and provenance. See SI 6 for detailed information, attributions, and frequencies of classification. See SI 7 for photographs of the archaeological specimen. See SI 2 for details about the dental anomalies. Refer to Fig. 2 and SI 5 for the distribution of centroid and isometric sizes in modern species and archaeological specimens. CCEC.51000004 is rather large for a *C. lupaster*. *Freq wild/dom* frequency of attribution between wild and domestic (step 2) during predictive LDA iterations (pldam); *Freq wild species* frequency of attribution between *C. lupus*, *C. lupaster*, and *L. mesomelas* (step 3) during predictive LDA iterations (pldam) on the specimens identified as wild; *CS* centroid size; *IS* isometric size; *DOG C. familiaris*; *WOLF C. lupus*; *LUPA C. lupaster*; *MESO L. mesomelas*. Previous determination: identification made by Louis Lortet and Claude Gaillard or written on the cranium

ID	Age	Dental anomalies	GMM 96.4% LDA Steps 2 and 3	Freq wild/dom	Freq wild species	CS	LMM 87.3% LDA	IS	Previous determination	Geographic provenance
CCEC.51000003	Subadult-juvenile	No	Wild-LUPA	100	98.5	0.43	Wild-LUPA	1.31	*Canis aureus*	?
CCEC.51000004	Young	No	Wild-LUPA	100	100	0.57	Wild-LUPA	1.55	*Canis doederleini* (Gaillard and Gaillard 1909: Fig. 202-203)	Assouan
CCEC.51000007	Adult	No	Wild-WOLF	100	100	0.55	Wild-WOLF	1.55	stray dog (Gaillard & Daressy, 1905: Fig. 4)	Roda
CCEC.51000008	Young	No	Domestic	100	/	0.51	Wild-LUPA	1.45		Assouan
CCEC.51000010	Young /adult	No	Wild-LUPA	100	100	0.56	Wild-WOLF	1.58	*Canis sacer* (Lortet and Gaillard 1907: Fig. 199-200)	Louqsor
CCEC.51000017	Young/adult	Yes	Domestic	100	/	0.54	Wild-LUPA	1.59	*Canis* sp	Tehneh
CCEC.51000031	Adult	Yes	Wild-LUPA	99.6	100	0.49	Domestic	1.45	*Canis* sp	?
CCEC.51000242	Adult	No	Domestic	100	/	0.49	Wild-LUPA	1.47	*Canis* sp	?
CCEC.90010304	Young/adult?	No	Wild-WOLF	100	77.25	0.59	Domestic	1.59	*Canis* sp	Tehneh
CCEC.90010309	Subadult	No	Wild-LUPA	100	100	0.46	Domestic	1.37	*Canis* sp	Roda
CCEC.90010310	Young/adult?	Yes	Domestic	100	/	0.51	Wild-WOLF	1.45	*Canis* sp	Roda
CCEC.90010311	Subadult	No	Wild-LUPA	100	100	0.49	Domestic	1.41	*Canis* sp	?

V. zerda (Castelló 2018, p. 207). Previous studies based on linear morphometrics have shown clear differences between Eurasian golden jackals and African golden wolves, yet morphometric comparisons of cranial shape between these species are scarce. Further research is, therefore, needed before a full evaluation of their presence or absence as mummified remains can be made. Additionally, the metadata on the modern sample did not allow us to account for sex or age differences. Due to the determinant role played by sexual dimorphism and ontogeny in cranial shape (Younes and Fouad 2016; Brassard 2020; Machado and Teta 2020), more modern specimens of known sex and age for each species are needed to build more accurate predictive models for example to apply on different age categories of archaeological remains.

Considering that some species have a low occurrence in our primary dataset (e.g. *C. aureus* is only represented by two specimens, Table 1), we preferred not to consider the full suite of species likely present in the study region, but rather to adopt a multi-step approach, by first determining the wild/domestic status of the ancient canids and then the species among those that were identified as wild after refining the list of species likely to be found in the wild archaeological sample. Indeed, LDA is very sensitive to sample size, and large differences in the number of specimens across groups may lead to the largest sample (i.e. dogs) dominating the pattern of variance–covariance in the data, resulting in a higher chance of assigning ancient specimen to these larger groups leading to a possible misinterpretation of classification accuracy (Kovarovic et al. 2011; Evin et al. 2013). To take into account all species in our balanced LDA, a larger and more robust sample is thus needed.

By considering large groups (i.e. domestic/wild and *C. lupus*/*C. lupaster*/*L. mesomelas*) in our analyses and performing analyses on balanced samples and on a subsample of the most discriminant PCs, we reduced the number of predictors to below that of the number of individuals of the smallest group and we ensured a satisfying number of specimens to define the reference groups in balanced analyses ($n = 100$ in analyses separating between domestic and wild, i.e. the number of dogs; and $n = 16$ in analyses on the candidate species only, i.e. number of *C. lupus*, Table 1). We can thus consider that our results are robust (Kovarovic et al. 2011). This is all the more important in the case of dogs, considering their tremendous diversity in cranial shape (which is as important as all wild species combined. This result is in line with those of Drake and Klingenberg (2010) who found that "the amount of shape variation among modern domestic dogs [much of which being the result of 200 years of intensive breeding] far exceeds that in modern wild species, and it is comparable to the disparity throughout the Carnivora"; Figs. 2 and 3). However, a larger sample for each wild species would be needed to provide a more accurate estimate of the precision of our method for wild canids.

Geometric versus linear morphometrics applied to archaeological remains

To date, Egyptologists have identified cranial remains based on macroscopic criteria (e.g. the relative size of the carnassial, which is unfortunately not always still present in the alveola, or tympanic bubble). Metrics appears useful to classify mummified remains more objectively and are necessary for the examination of large datasets. In this study, we demonstrated that 3D geometric morphometrics is a very powerful method for determining whether ancient mummified canids were domestic dogs or wild canids. In addition, we found it is much more accurate (with a degree of confidence of over 97%) than linear morphometrics (88%). Linear morphometrics is thus not sufficient, and 3D geometric methods undoubtedly bring an additional refinement for the identification of species and for estimating wild/domestic ratios in large assemblages. We also obtained very satisfying results when determining species among wild canids for a subset of taxa that more closely resembled the ancient specimens (*C. lupaster*, *C. lupus*, *L. mesomelas*, CVP of over 96%).

Problematic identifications between extant dogs and grey wolves and among extant *C. lupus*, *C. lupaster*, and *C. mesomelas*

Several factors may explain why some wolves were identified as dogs in our modern reference sample and why the distinction between some *C. lupus*, *C. lupaster*, and *C. mesomelas* remains difficult. First, recent changes in the classification (and the ongoing evolution of taxonomic considerations, as raised in the introduction) made the constitution of the reference sample challenging. Second, some wild canid species are very similar in shape (see SI 1) due to strong morphological convergence, with specimens displaying remarkably similar phenotypes to the point of being mistaken by trained biologists. This may explain our difficulties in distinguishing between *C. lupus*, *C. lupaster*, and *C. mesomelas* or between *V. pallida* and *V. rueppelli*. Moreover, it is not impossible that some modern specimens from the collections were originally misidentified, thus biasing the results of our predictive models. In our study, *C. lupaster* occupies an intermediate and overlapping morphospace position (Figs. 2 and 4B) between jackal-like forms and wolf-like forms, as found in previous studies (Machado and Teta 2020). These morphological similarities are in line with previous GMM studies that showed important variation within *Canis lupaster*, with some subspecies showing morphological convergence with other species (e.g. between *C. l. soudanicus* and *L. adusta*, or between *C. l. bea*, *L. mesomeleas*, and *C. aureus*). A

robust species determination can be postulated by considering the species ' current African or Near Eastern distribution (when not sympatric), but this cannot be definitive since it presumes that species ranges and distributions have not changed over time. A third significant challenge hinges on the fact that sympatric members of the genus *Canis* can readily hybridize in the wild, and that some of those hybrids are viable and able to form taxonomic complexes that are "ecologically and morphologically distinct from their parent species" (Gopalakrishnan et al. 2018; Machado and Teta 2020). Past hybridization and admixture between domestic and wild canids have been proven, for example between dogs and the African golden wolf (Bahlk 2015; Mallil et al. 2020), golden jackals (Galov et al. 2015), or Iranian wolves (*C. lupus pallipes*; Khosravi et al. 2013). The roaming of feral dogs in ancient Egypt may have promoted this hybridization and could explain why some ancient specimens were more difficult to classify between domestic and wild types. Other studies have identified gene flow between Eurasian golden jackals from Israel and grey wolves, dogs, and the African golden wolf (Koepfli et al. 2015), and between the Ethiopian wolf (*C. simensis*) and the African golden wolf (Bahlk 2015). Some studies have even suggested that the African golden wolf may originate from the hybridization between grey and Ethiopian wolves (Gopalakrishnan et al. 2018).

None of these limitations regarding species identification necessarily represent a major obstacle for studies of mummified canid remains. On the one hand, ancient Egyptians had a different concept of species classification than we do (Charron 2002). On the other, what also interests us is to obtain information on the supply strategies/sourcing of the animals and related insights into mummification practises in conjunction with religious beliefs. Therefore, the most important classification to be made is between domestic and wild, and the method we outline here is excellent at doing so.

Domestic versus wild and identification of wild canids in the ancient mummies of the *Musée des Confluences*

Among the isolated crania of canid mummies from the Musée des Confluences, based on geometric morphometrics, we identified mainly dogs ($N=33$), but also eight wild canids, belonging to either Near Easter grey wolves ($N=2$) or African golden wolves ($N=6$). Ancient DNA analyses would be necessary, however, to confirm our final determinations and thus assess the reliability of the 3D GMM method when applied to ancient remains. All specimens were classified in the domestic or wild group and then to *C. lupus* or *C. lupaster* with high probability (considering the CVPs in steps 1 and 2 and the number of similar attributions through the 1000 balanced LDAs on a randomly selected balanced sample, see SI 6). Only the case of CCEC.90010304 leads to confusion between grey and golden wolf, yet the centroid size tends to support the attribution to a grey wolf.

The identification of specimen CCEC.510000031 as a *C. lupaster* was somewhat unexpected, because this cranium shows traits that led us to classify it as a dog at first sight (see SI 7). However, the slightly depressed frontal bones and very developed zygomatic processes (somewhat abnormally) may have biased our qualitative determination. This individual could also be a hybrid, or an animal taken from the wild and then bred in captivity. Our identification for this specimen is thus to be taken with caution pending further analysis of other available bones, such as the mandible. We may note that this specimen was the only one among all those attributed to the wild group to present dental pathologies (Table 4, SI 2), whilst six ancient canids identified as domestic had dental anomalies (see SI 2 and SI 6). The cranium CCEC.510000031 indeed showed an advanced degree of dental wear and signs of advanced periodontitis, with osteolysis at the root of the molars and oronasal fistula (SI 8). Although periodontitis is often more severe in domestic dogs (Harvey 1998) or captive animals, it is also described in the wild. Bertè (2017) has described similar traits in a specimen of *C. lupaster* caught from the wild at the oasis of Giarabub (specimen MSNG 26228, collected in 1926–1927 by C. Confalonieri; Bertè 2017). Other studies also support that tooth crowding and dental anomalies are not a proper sign of domestication (e.g.Janssens et al. 2016; Ameen et al. 2017).

One of the mummified canids identified as an African golden wolf (*C. lupaster*) is from Roda, others are from Assouan and Louqsor (Table 4). Those identified as grey wolves (*C. lupus*) are from Roda and Tehneh. Unfortunately, due to the inconsistent recovery and curation practises of the early twentieth century, the specimens hosted in many museum collections are rarely properly contextualized (the provenance is not even always known), limiting our interpretations. It will thus be crucial to study specimens from the field to go beyond the simple determination and description and provide conclusions on the sourcing of the animals. To our knowledge, this is the first study to consider the presence of Near Eastern wolves among canid mummies. It will be necessary to enrich both our modern and archaeological databases prior to questioning deeper the use of this species for mummification.

Although 3D GMM is efficient for species determination, this method should be seen as complementary to the qualitative/morphoscopic approach, since it only partially captures shape compared to the human eye. Our own results may have been better had we used sliding semi-landmarks on curves and surface landmarks (i.e. landmarks placed on the whole external surface of the skull). However, this would have allowed us to capture only the skulls with an intact surface, thus reducing our sample size. We instead considered

only a limited number of anatomical landmarks to be able to include also crania with a slightly damaged surface (including crania which retained residues of mummified tissue; see example in SI 7). Due to the special nature of the materials under study, we were fortunate enough to have access to significant numbers of complete crania, an uncommon feature of most zooarchaeological collections. Three-dimensional GMM methods can also be applied to fragmented remains more efficiently than linear morphometrics, and we could easily adapt the landmarking protocol to different fragmentation patterns to include more specimens in the analyses, using a subset of the landmarks considered in this paper (for example see Brassard et al. 2022). Moreover, we only analyzed isolated crania, but 3D models could be obtained from medical scanners to access the data without the need to unwrap the mummy. Building 3D archives of the specimens allows moreover to later observe additional macroscopic or quantitative characters not considered in the current study and will facilitate future data sharing (Spyrou et al. 2022).

Conclusions and future perspectives

Geometric morphometrics provides a more efficient way of identifying crania in mummified canids from Ancient Egypt compared to traditional linear morphometrics. Based on a sample of 100 modern dogs and 157 modern specimens of 13 wild species from Africa and the Near or Middle East, predictive methods applied to the shape of their cranium allowed to determine the domestic status of ancient mummies and the wild species among *C. lupaster*, *C. lupus*, and *L. mesomelas* with a probability over 96%. However, the reference sample we used needs to be further expanded to ensure it better represents the full diversity of shapes in wild canids. The results provided in this article strongly encourage the use of landmark-based 3D geometric morphometrics for a more reliable determination of ancient canids, not only in Ancient Egyptian contexts but also for the identification of ancient remains whose identification is unclear.

Our results revealed that the majority of mummified canids in this dataset were the remains of domestic dogs. Ancient DNA analyses could be deployed on the same specimens to cross-validate the results with the predictions based on 3D GMM in order to assess the reliability of our method. Once confirmed, the next step would be to increase the sample with specimens from contextualized sites, by photographing skulls in situ in dog catacombs. It will be then possible to further quantify the diversity in mummified canids and that of ancient dogs to explore whether, for example, some particular morphologies were favoured over others, or if assumptions can be made on their living condition (feral, captivity), thus opening new perspectives pertaining to the source of canids used for mummification.

Close-range photogrammetry, as used here, is a relatively easy and low-cost technique to reconstruct geometrically accurate 3D models of specimens in situ, i.e. in dog catacombs, to further explore the diversity in mummified canids in contextualized sites. It is now widely used in archaeology (e.g. Drake et al. 2015; Evin et al. 2016; Hanot et al. 2017; Harbers et al. 2020; Neaux et al. 2021; Brassard et al. 2022; Spyrou et al. 2022) and can be applied to objects of all size as long as photographs of the object can be obtained under different orientations, for example by turning around the specimen or placing it on a turning table. Specifically, for canids, protocols for 3D model acquisition in the field and later reconstruction after fieldwork are available (e.g. Evin et al. 2016 or this study: see SI 10) and can greatly complement traditional observations and measurements even though they require more time. Moreover, it allows the safeguarding and sharing of ancient remains that one is not sure to find across different field campaigns. In addition, new 3D printing technologies allow to duplicate the ancient remains via their numerical models which can be used for display in for example museums or used for outreach activities.

Supplementary Information The online version contains supplementary material available at https://doi.org/10.1007/s12520-023-01760-1.

Acknowledgements We thank Museums for providing access to their collections, in particular Didier Berthet and the Centre Louis Lortet – Musée des Confluences (Lyon, France), Géraldine Véron and the Muséum national d'Histoire naturelle (Paris, France), Stefan Hertwig and the Naturhistorische Museum Bern (Bern, Switzerland), Daniela Schweizer and the Vetsuisse Faculty of the University of Bern (Switzerland), Christiane Funk and the Museum für Naturkunde—Leibniz Institute for Evolution and Biodiversity Science (Berlin, Germany), Emmanuel Gilissen and the RMCA Museum, and the Harvard Museum of Comparative Zoology. We thank Anne-Claire Fabre for providing 3D models of specimens and people who provided access to surface or CT scan facilities (including Anthony Herrel and the University Hospital in Jena, Germany) or financial support for some of the 3D acquisitions (including Greger Larson). AE received funding from the European Research Council (ERC) under the European Union's Horizon 2020 research and innovation program (Grant Agreement No. 852573). We are very grateful to Anthony Herrel and two anonymous reviewers for proofreading this manuscript.

Author contributions C. B. conceptualized the project, set up the study, acquired data, performed the statistical analyses, and wrote the first draft of the manuscript. A. E., A. C., S. C., M. M., and D. T. provided 3D models for shape analyses. H. J. and C. G. collected part of the material and gave access to it. A. E. gave advise for the statistical analyses and was a major contributor in analyzing the data. H. J. is responsible for project administration and supervision. The manuscript was edited by C. B., A. E., A. C., S. C., M. M., D. T., K. D., and S.P. All authors gave final approval for publication and agreed to be held accountable for the work performed therein.

Funding The research leading to these results received funding from the Fyssen foundation, the 'investissement d'avenir' project Labex BCDiv (10-LABX-003), and the European Research Council (Grant Agreement No. 852573).

Data availability All data generated or analyzed during this study are included in this published article (and its supplementary information files). All three-dimensional models of the crania are available in SI 9. Detailed information about the sample and methods are provided in SI 2. Raw 3D coordinates of the landmarks considered in GMM analyses are in SI 3.

Code availability The R code is available from C. B. on request.

Declarations

Ethics approval Not applicable.

Consent to participate Not applicable.

Consent for publication Not applicable.

Competing interests The authors declare no competing interests.

References

Abdelaziz M, Elsayed M (2019) Underwater photogrammetry digital surface model (DSM) of the submerged site of the ancient lighthouse near Qaitbay fort in Alexandria, Egypt. Int Arch Photogramm Remote Sens Spat Inf Sci XLII-2/W10:1–8. https://doi.org/10.5194/ISPRS-ARCHIVES-XLII-2-W10-1-2019

Adams DC, Collyer M, Kaliontzopoulou A, Sherratt E (2016) Geomorph: software for geometric morphometric analyses

Ameen C, Hulme-Beaman A, Evin A et al (2017) A landmark-based approach for assessing the reliability of mandibular tooth crowding as a marker of dog domestication. J Archaeol Sci 85:41–50. https://doi.org/10.1016/j.jas.2017.06.014

Ameen C, Feuerborn TR, Brown SK et al (2019) Specialized sledge dogs accompanied Inuit dispersal across the North American Arctic. Proc R Soc B Biol Sci 286:20191929. https://doi.org/10.1098/rspb.2019.1929

Bahlk SH (2015) Can hybridization be detected between African wolves and sympatric canids? Master of Science thesis, University of Oslo, Norway

Barone R (2010) Anatomie comparée des mammifères domestiques : Tome 1, Ostéologie, 5e édition. Vigot, Paris

Baylac M, Frieß M (2005) Fourier descriptors, Procrustes superimposition, and data dimensionality: an example of cranial shape analysis in modern human populations. In: Slice DE (ed) Modern Morphometrics in Physical Anthropology. Springer, US, Boston, MA, pp 145–165

Bertè DF (2017) Remarks on the skull morphology of Canis lupaster Hemprich and Herenberg, 1832 from the collection of the Natural History Museum "G. Doria" of Genoa. Italy Nat Hist Sci 4:19–29. https://doi.org/10.4081/nhs.2017.318

Bookstein FL (1989) Principal warps: thin-plate splines and the decomposition of deformations. IEEE Trans Pattern Anal Mach Intell 11:567–585. https://doi.org/10.1109/34.24792

Bookstein FL (1991) Morphometric tools for landmark data. Cambridge University Press, Geometry and Biology

Bouvier-Closse K (2003) Les noms propres de chiens, chevaux et chats de l'Égypte ancienne. Le rôle et le sens du nom personnel attribué à l'animal. Anthropozoologica 37:11–38

Brassard C, Callou C, Porcier S (2021) To be or not to be a dog mummy: how a metric study of the skull can inform on selection practices pertaining to canid mummification in Ancient Egypt In: The Ancient Egyptians & the Natural World. Sidestone Press, Cairo, Egypt

Brassard C, Bălăşescu A, Arbogast R-M et al (2022) Unexpected morphological diversity in ancient dogs compared to modern relatives. Proc R Soc B Biol Sci 289:20220147. https://doi.org/10.1098/rspb.2022.0147

Brassard C (2017) Le chien en Egypte ancienne : approche archéozoologique et apports de la craniologie. Application a une série de chiens momifiés (El-Deir) et comparaison avec des chiens actuels et anciens (Kerma). Thesis of veterinary medicine, Vetagro Sup campus vétérinaire de Lyon, Université Claude-Bernard Lyon 1

Brassard C (2020) Morphological variability in dogs and red foxes from the first European agricultural societies: a morpho-functional approach based on the mandible. PhD thesis, Muséum national d'Histoire naturelle

Brémont A (2021) Newcomers in the bestiary. A review of the presence of Lycaon pictus in Late Predynastic and Early Dynastic Environment and Iconography In: The Ancient Egyptians and the Natural World, Sidestone Press, Cairo, Egypt

Brixhe J (2019) Le chien dans l'Egypte ancienne: les origines. Pharaon, Le magazine de l'Egypte éternelle 21, pp. 31–34

Castelló JR (2018) Canids of the world: wolves, wild dogs, foxes, jackals, coyotes, and their relatives. Princeton University Press

Charron A (2002) Taxonomie des espèces animales dans l'Egypte gréco-romaine. Bulletin de la Société française d'Egyptologie 156, pp. 7–19

Cignoni P, Callieri M, Corsini M, et al (2008) MeshLab: an Open-Source Mesh Processing Tool. Computing. 1. 129–136. https://doi.org/10.2312/LocalChapterEvents/ItalChap/ItalianChapConf2008/129-136

Claude J (2013) Log-shape ratios, Procrustes superimposition, elliptic Fourier analysis: three worked examples in R. Hystrix Ital J Mammal 24:94–102. https://doi.org/10.4404/hystrix-24.1-6316

Collyer ML, Sekora DJ, Adams DC (2015) A method for analysis of phenotypic change for phenotypes described by high-dimensional data. Heredity 115:357

Drake AG, Klingenberg CP (2010) Large-scale diversification of skull shape in domestic dogs: disparity and modularity. Am Nat 175:289–301. https://doi.org/10.1086/650372

Drake AG, Coquerelle M, Colombeau G (2015) 3D morphometric analysis of fossil canid skulls contradicts the suggested domestication of dogs during the late Paleolithic. Sci Rep 5:82–99. https://doi.org/10.1038/srep08299

Drake AG, Coquerelle M, Kosintsev PA et al (2017) Three-dimensional geometric morphometric analysis of fossil canid mandibles and skulls. Sci Rep 7:9508. https://doi.org/10.1038/s41598-017-10232-1

Dryden IL, Mardia KV (2016) Statistical shape analysis: with applications in R. John Wiley & Sons

Dunand F, Lichtenberg R, Charron A (2005) Des animaux et des hommes: une symbiose égyptienne. Editions du rocher, Monaco, France

Dunand F, Lichtenberg R, Callou C, Willemin FL (2017) El-Deir nécropoles: Les chiens momifiés d'El-Deir IV. Cybele Editions

Durisch Gauthier N (2002) Anubis et les territoires cynopolites selon les temples ptolémaïques et romains. PhD thesis, University of Geneva, Switzerland

Evin A, Cucchi T, Cardini A et al (2013) The long and winding road: identifying pig domestication through molar size and shape. J Archaeol Sci 40:735–743. https://doi.org/10.1016/j.jas.2012.08.005

Evin A, Flink LG, Bălăşescu A et al (2015) Unravelling the complexity of domestication: a case study using morphometrics and ancient DNA analyses of archaeological pigs from Romania. Philos Trans R Soc B Biol Sci. https://doi.org/10.1098/rstb.2013.0616

Evin A, Souter T, Hulme-Beaman A et al (2016) The use of close-range photogrammetry in zooarchaeology: creating accurate 3D models of wolf crania to study dog domestication. J Archaeol Sci Rep 9:87–93. https://doi.org/10.1016/j.jasrep.2016.06.028

Evin A, Bonhomme V, Claude J (2020) Optimizing digitalization effort in morphometrics. Biol Methods Protoc 5:bpaa023. https://doi.org/10.1093/biomethods/bpaa023

Evin A, Bouby L, Bonhomme V, et al (2022) Archaeophenomics of ancient domestic plants and animals using geometric morphometrics : a review. Peer Community J 2:. https://doi.org/10.24072/pcjournal.126

Fabre A-C, Cornette R, Huyghe K et al (2014) Linear versus geometric morphometric approaches for the analysis of head shape dimorphism in lizards. J Morphol 275:1016–1026. https://doi.org/10.1002/jmor.20278

Fau M, Cornette R, Houssaye A (2016) Photogrammetry for 3D digitizing bones of mounted skeletons: potential and limits. CR Palevol 15:968–977. https://doi.org/10.1016/j.crpv.2016.08.003

Foote M (1997) The Evolution of morphological diversity. Annu Rev Ecol Syst 28:129–152

Forbes-Harper JL, Crawford HM, Dundas SJ et al (2017) Diet and bite force in red foxes: ontogenetic and sex differences in an invasive carnivore. J Zool 303:54–63. https://doi.org/10.1111/jzo.12463

Gaillard C, Daressy (1905) La faune momifiée de l'antique Egypte, Catalogue général des Antiquités égyptiennes du Musée du Caire

Galov A, Fabbri E, Caniglia R et al (2015) First evidence of hybridization between golden jackal (*Canis aureus*) and domestic dog (*Canis familiaris*) as revealed by genetic markers. R Soc Open Sci 2:150450. https://doi.org/10.1098/rsos.150450

Goodall C (1991) Procrustes methods in the statistical analysis of shape. J R Stat Soc Ser B Methodol 53:285–321

Gopalakrishnan S, Sinding M-HS, Ramos-Madrigal J et al (2018) Interspecific gene flow shaped the evolution of the genus Canis. Curr Biol 28:3441-3449.e5. https://doi.org/10.1016/j.cub.2018.08.041

Hanot P, Guintard C, Lepetz S, Cornette R (2017) Identifying domestic horses, donkeys and hybrids from archaeological deposits: a 3D morphological investigation on skeletons. J Archaeol Sci 78:88–98. https://doi.org/10.1016/j.jas.2016.12.002

Harbers H, Neaux D, Ortiz K et al (2020) The mark of captivity: plastic responses in the ankle bone of a wild ungulate (Sus scrofa). R Soc Open Sci 7:192039

Hartley ML (2017) Paws in the sand: the emergence and development of the use of canids in the funerary practice of the ancient Egyptians (ca. 5000 BC–395 AD). PhD thesis, Macquarie University, Australia

Harvey CE (1998) Periodontal disease in dogs: etiopathogenesis, prevalence, and significance. Vet Clin North Am Small Anim Pract 28:1111–1128. https://doi.org/10.1016/S0195-5616(98)50105-2

Ikram S (2013) Man's best friend for eternity: dog and human burials in Ancient Egypt. Anthropozoologica 48:299–307. https://doi.org/10.5252/az2013n2a8

Janssens L, Verhaert L, Berkowic D, Adriaens D (2016) A standardized framework for examination of oral lesions in wolf skulls (Carnivora: Canidae: Canis lupus). J Mammal 97:1111–1124. https://doi.org/10.1093/jmammal/gyw058

Jeanjean M, Haruda A, Salvagno L et al (2022) Sorting the flock: quantitative identification of sheep and goat from isolated third lower molars and mandibles through geometric morphometrics. J Archaeol Sci 141:105580. https://doi.org/10.1016/j.jas.2022.105580

Khosravi R, Rezaei HR, Kaboli M (2013) Detecting hybridization between Iranian wild wolf (Canis lupus pallipes) and free-ranging domestic dog (Canis familiaris) by analysis of microsatellite markers. Zoolog Sci 30:27–34. https://doi.org/10.2108/zsj.30.27

Kitagawa C (2016) The tomb of the dogs at Asyut: faunal remains and other selected objects. Harrassowitz Verlag, Wiesbaden

Klingenberg CP (2016) Size, shape, and form: concepts of allometry in geometric morphometrics. Dev Genes Evol 226:113–137. https://doi.org/10.1007/s00427-016-0539-2

Koepfli K-P, Pollinger J, Godinho R et al (2015) Genome-wide evidence reveals that African and Eurasian golden jackals are distinct species. Curr Biol 25:2158–2165. https://doi.org/10.1016/j.cub.2015.06.060

Kovarovic K, Aiello LC, Cardini A, Lockwood CA (2011) Discriminant function analyses in archaeology: are classification rates too good to be true? J Archaeol Sci 38:3006–3018. https://doi.org/10.1016/j.jas.2011.06.028

Lima RD, Sykora T, Meyer MD, et al (2018) On combining epigraphy, TLS, photogrammetry, and interactive media for heritage documentation: the case study of Djehutihotep's tomb in Dayr al-Barsha. Eurographics Workshop Graph Cult Herit 5 pages. https://doi.org/10.2312/GCH.20181367

Lortet L, Gaillard C (1903) La faune momifiée de l'Ancienne Egypte et recherches anthropologiques, 1ère série, Archives du Muséum d'Histoire naturelle de Lyon, 8

Lortet L, Gaillard C (1907) La faune momifiée de l'Ancienne Egypte et recherches anthropologiques, 2ème série, Archives du Muséum d'Histoire naturelle de Lyon, 9

Lortet L, Gaillard C (1909) La faune momifiée de l'Ancienne Egypte et recherches anthropologiques, 3-4-5 ème séries, Archives du Muséum d'Histoire naturelle de Lyon, 10

Machado FA, Teta P (2020) Morphometric analysis of skull shape reveals unprecedented diversity of African Canidae. J Mammal 101:349–360. https://doi.org/10.1093/jmammal/gyz214

Mallil K, Justy F, Rueness EK et al (2020) Population genetics of the African wolf (Canis lupaster) across its range: first evidence of hybridization with domestic dogs in Africa. Mamm Biol 100:645–658. https://doi.org/10.1007/s42991-020-00059-1

Manin A, Evin A (2020) Canis spp. identification in central Mexico and its archaeological implications : toward a better understanding of the ecology and the cultural role of canids in ancient MesoAmerica In: Boudadi-Maligne, Myriam, Mallye, Jean-Baptiste (ed) Relations hommes – canidés de la préhistoire aux périodes modernes, Pessac, Ausonius editions, pp. 94–114. http://dx.doi.org/10.46608/DANA3.9782381490120.6

Mitteroecker P, Bookstein F (2011) Linear discrimination, ordination, and the visualization of selection gradients in modern morphometrics. Evol Biol 38:100–114. https://doi.org/10.1007/s11692-011-9109-8

Mitteroecker P, Gunz P (2009) Advances in Geometric Morphometrics. Evol Biol 36:235–247. https://doi.org/10.1007/s11692-009-9055-x

Mosimann JE (1970) Size allometry: size and shape variables with characterizations of the lognormal and generalized gamma distributions. J Am Stat Assoc 65:930–945. https://doi.org/10.1080/01621459.1970.10481136

Murnane W, Ikram S, Dodson A (2000) The mummy in Ancient Egypt: equipping the dead for eternity. J Am Orient Soc 120:97. https://doi.org/10.2307/604889

NAV (2017) Nomina Anatomica Veterinaria, 6th Edition, Word Association of Veterinary Anatomists (W.A.V.A.)

Neaux D, Blanc B, Ortiz K et al (2021) How changes in functional demands associated with captivity affect the skull shape of a wild boar (Sus scrofa). Evol Biol 48:27–40

Osborn DJ, Osbornová J (1998) The mammals of ancient Egypt. Aris & Phillips, Warminster

Parés-Casanova PM, Salamanca-Carreño A, Crosby-Granados RA, Bentez-Molano J (2020) A comparison of traditional and geometric morphometric techniques for the study of basicranial morphology in horses: a case study of the Araucanian horse from Colombia. Anim Open Access J MDPI 10:E118. https://doi.org/10.3390/ani10010118

Porcier SM, Berruyer C, Pasquali S et al (2019) Wild crocodiles hunted to make mummies in Roman Egypt: evidence from synchrotron imaging. J Archaeol Sci 110:105009. https://doi.org/10.1016/j.jas.2019.105009

Prada L, Wordsworth PD (2018) Evolving epigraphic standards in the field: documenting Late Period and Graeco-Roman Egyptian graffiti through photogrammetry at Elkab. In: Hoogendijk FAJ and van Gompel S (ed) The Materiality of Texts from Ancient Egypt, pp. 76–93. Brill. https://doi.org/10.1163/9789004375277_009

R Core Team (2021) R: a language and environment for statistical computing. R Foundation for Statistical Computing, Vienna, Austria

Richardin P, Porcier S, Ikram S et al (2017) Cats, crocodiles, cattle, and more: initial steps toward establishing a chronology of Ancient Egyptian animal mummies. Radiocarbon 59:595–607. https://doi.org/10.1017/RDC.2016.102

Roberts T, McGreevy P, Valenzuela M (2010) Human induced rotation and reorganization of the brain of domestic dogs. Plos One 5:e11946. https://doi.org/10.1371/journal.pone.0011946

Rohlf F, Slice D (1990) Extensions of the Procrustes method for the optimal superimposition of landmarks. Syst Zool 39:40–59. https://doi.org/10.2307/2992207

Rouvière L (2017) Le culte des canidés dans la région de Hardaï/Cynopolis. Enquête épigraphique et archéologique, In: Cassier C (éd.) Géographie et archéologie de la religion égyptienne. Espaces cultuels, pratiques locales, CENiM 17, p. 109–128.

Rueness EK, Asmyhr MG, Sillero-Zubiri C et al (2011) The cryptic African Wolf: Canis aureus lupaster is not a golden jackal and is not endemic to Egypt. Plos One 6:e16385. https://doi.org/10.1371/journal.pone.0016385

Saleh M, Younes M, Basuony A et al (2018) Distribution and phylogeography of Blanford's Fox, Vulpes cana (Carnivora: Canidae), in Africa and the Middle East. Zool Middle East 64:9–26. https://doi.org/10.1080/09397140.2017.1419454

Schenkel W (1963) Die Farben in ägyptischer Kunst und Sprache. Z Für Ägyptische Sprache Altertumskunde 88:131–147. https://doi.org/10.1524/zaes.1963.88.jg.131

Schenkel W (2007) Color terms in ancient Egyptian and Coptic. In: MacLaury RE, Paramei GV, Dedrick D (eds) Anthropology of Color. John Benjamins Publishing Company, Amsterdam, pp 211–228

Schlager S (2017) Chapter 9 - Morpho and Rvcg – Shape Analysis in R: R-Packages for Geometric Morphometrics, Shape Analysis and Surface Manipulations. In: Zheng G, Li S, Székely G (eds) Statistical Shape and Deformation Analysis. Academic Press, pp 217–256

Spyrou A, Nobles G, Hadjikoumis A et al (2022) Digital zooarchaeology: state of the art, challenges, prospects and synergies. J Archaeol Sci Rep 45:103588. https://doi.org/10.1016/j.jasrep.2022.103588

Thiringer M (2020) An Egyptian's best friend? An analysis and discussion of the depiction of the domestic dog in Ancient Egypt. PhD thesis, University of Memphis, USA

Vasilyev S, Vasilyeva O, Galeev R, et al (2019) 3D reconstruction of the Ancient Egyptian mummy skeleton from the Pushkin State Museum of Fine Arts (I,1 1240). ISPRS - Int Arch Photogramm Remote Sens Spat Inf Sci XLII-2/W12:225–229. https://doi.org/10.5194/isprs-archives-XLII-2-W12-225-2019

Viranta S, Atickem A, Werdelin L, Stenseth NChr, (2017) Rediscovering a forgotten canid species. BMC Zool 2:6. https://doi.org/10.1186/s40850-017-0015-0

von den Driesch A (1976) A guide to the measurement of animal bones from archaeological sites. Vol. 1, Peabody Museum Press, Cambridge

Wiley DF, Amenta N, Alcantara DA, et al (2005) Evolutionary morphing. IEEE Visualization, Minneapolis, USA, pp. 431–438. https://doi.org/10.1109/VISUAL.2005.1532826

Wilson D, Reeder D (2005) Mammal species of the world: a taxonomic and geographic reference. 3rd edition. Johns Hopkins University Press, Baltymore, Maryland, USA

Younes MI, Fouad F (2016) Cranial allometry, sexual dimorphism and age structure in sample of the Egyptian wolf canisanthuslupaster. Al-Azhar Bull Sci 27:1–8

Yoyotte J, Charvet P, Gompertz S (1997) Le voyage en Egypte: un regard romain / Strabon, NiL Éd

Zelditch ML, Swiderski DL, Sheets HD (2012) Geometric morphometrics for biologists: a primer. Academic Press

Authors and Affiliations

C. Brassard[1,2] · A. Evin[3] · C. Ameen[4] · S. Curth[5] · M. Michaud[6] · D. Tamagnini[7,8] · K. Dobney[9,10,11,12] · C. Guintard[13,14] · S. Porcier[15] · H. Jerbi[16]

1 Fondation Fyssen, 194 Rue de Rivoli, 75001 Paris, France

2 MECADEV-UMR 7179, Muséum National d'Histoire Naturelle, 75005 Paris, France

3 ISEM, University of Montpellier, CNRS, EPHE, IRD, Montpellier, France

4 Department of Archaeology, University of Exeter, Exeter EX4 4QE, UK

5 Aquazoo Löbbecke Museum, Kaiserswerther Straße 380, 40474 Düsseldorf, Germany

6 Department of African Zoology, Royal Museum for Central Africa, Tervuren, Belgium

7 Department of Biology and Biotechnologies "Charles Darwin", University of Rome "La Sapienza", Rome, Italy

8 Museum of Zoology, Sapienza Museum Centre, University of Rome "La Sapienza", Building, Viale Dell'Universita 32, 00185 Rome, Italy

9 Department of Archaeology, School of Philosophical and Historical Inquiry (SOPHI), Faculty of Arts and Social Sciences, University of Sydney, Sydney, Australia

10 Department of Archaeology, Classics and Egyptology, University of Liverpool, University of Liverpool, 12-14 Abercromby Square Liverpool, Liverpool L69 7WZ, UK

11 Department of Archaeology, Univeristy of Aberdeen, St Mary's Building, Elphinstone Road, Aberdeen AB24 3UF, UK

12 Department of Archaeology, Simon Fraser University, Burnaby, B.C. V5A 1S6, Canada

13 Laboratoire d'Anatomie Comparée, Ecole Nationale Vétérinaire, de l'Agroalimentaire Et de L'Alimentation, Nantes Atlantique – ONIRIS, Nantes Cedex 03, France

14 GEROM, UPRES EA 4658, LABCOM ANR NEXTBONE, Faculté de Santé de L'Université d'Angers, Angers, France

15 ASM-UMR 5140, University of Paul-Valéry Montpellier 3, LabexARCHIMEDE, Montpellier, France

16 Service d'anatomie, Ecole Nationale de Médecine Vétérinaire Sidi Thabet, CP2020 Sidi Thabet, Tunisia